Electrosynthesized molecularly imprinted polyscopoletin nanofilms for human serum albumin detection

Zorica Stojanovic[a], Júlia Erdőssy[b], Katalin Keltai[c], Frieder W. Scheller[d], Róbert E. Gyurcsányi[b*]

[a] University of Novi Sad, Faculty of Technology, Department of Applied and Engineering Chemistry, Bul. cara Lazara 1, 21000, Novi Sad, Serbia

[b] MTA-BME "Lendület" Chemical Nanosensors Research Group, Department of Inorganic and Analytical Chemistry, Budapest University of Technology and Economics, Szent Gellért tér 4, H-1111 Budapest, Hungary

[c] Department of Internal Medicine, Faculty of Medicine, Semmelweis University, Kútvölgyi út 4, H-1125 Budapest, Hungary

[d] Institute of Biochemistry and Biology, University of Potsdam, Karl-Liebknecht-Strasse 25-26, Potsdam D-14476, Germany

*Corresponding author: robertgy@mail.bme.hu

Abstract

Molecularly imprinted polymers (MIPs) rendered selective solely by the imprinting with protein templates lacking of distinctive properties to facilitate strong target-MIP interaction are likely to exhibit medium to low template binding affinities. While this prohibits the use of such MIPs for applications requiring the assessment of very low template concentrations, their implementation for the quantification of high-abundance proteins seems to have a clear niche in the analytical practice. We investigated this opportunity by developing a polyscopoletin-based MIP nanofilm for the electrochemical determination of elevated human serum albumin (HSA) in urine. As reference for low abundance protein ferritin-MIPs were

also prepared by the same procedure. Under optimal conditions, the imprinted sensors gave a linear response to HSA in the concentration range of 20-100 mg/dm^3, and to ferritin in the range of 120-360 mg/dm^3. While as expected the obtained limit of detection was not sufficient to determine endogenous ferritin in plasma, the HSA-sensor was successfully employed to analyse urine samples of patients with albuminuria. The results suggest that MIP-based sensors may be applicable for quantifying high abundance proteins in a clinical setting.

Keywords: Human serum albumin; ferritin; molecularly imprinted polymer; scopoletin; urine

1. INTRODUCTION

Since the fragility of antibodies is limiting in many biosensing applications their replacement with more robust selective receptors received considerable attention.[1] In this respect general synthetic processes with broad applicability in terms of targets to be recognized such as molecular imprinting of polymers are especially appealing.[2, 3] Molecular imprinting uses the target as a template during polymerization of functional monomers. Subsequent removal of the template leads to recognition sites in the molecularly imprinted polymer (MIP) that can selectively rebind the target. Extending this principle to macromolecules such as proteins necessitated the implementation of a variety of enabling technologies (e.g., epitope imprinting,[4, 5] surface imprinting[6-10]) to cope both with the fragility of the target[11] as well as with its limited diffusivity in the cross-linked polymeric matrices. The electrochemical polymerization in this respect offers clear advantages such as performing the polymerization in aqueous conditions that is compatible with the proteinaceous target. Moreover, in terms of chemical sensor fabrication it enables the controlled deposition of MIP nanofilms directly onto an electrode surface.[12-14] While the molecular imprinting concept is fairly universal the functional monomers to provide selective recognition are not, i.e., the library of monomers is rather limited and monomers adequate for a certain protein target may not be necessarily optimal for another.[15] While high affinity MIPs were reported for a number of targets[16, 17], the selectivity of protein-MIPs is often enhanced by incorporating in the MIPs compounds known to interact with the target, e.g. substrates or inhibitors of an enzyme target[18, 19], aptamers[20] and various nanomaterials[16, 21]. Alternatively, rational design of monomers tuned for the specific target and semi-covalent imprinting was also shown to give MIPs with high affinity towards protein templates [22].

However, target specific tuning of the molecular imprinting process departs from the basic universal concept, i.e., to obtain a polymer rendered selective towards different proteins

solely by the molecular imprinting process. The difficulty to achieve this goal is largely due to the lack of universally applicable monomer library, i.e., in case of electropolymerized MIPs generally only a single monomer is used for the synthesis of MIPs.[15] Given the diversity of proteins in terms of physical chemical properties it is unlikely to have the full range of interactions for high affinity binding covered by these simple MIPs. Therefore, the success rate of this probabilistic approach was increased in many cases by focusing on proteins with distinctive properties[8, 23] that facilitates the likelihood of obtaining binding sites with both strong and selective interaction with the target. However, for "random" protein targets lacking such properties the resulting MIPs rendered selective solely by imprinting are likely to exhibit low to medium affinities, which prohibits their use for practical application where low or even trace amounts of proteins need to be detected. Still their implementation for the recognition of high-abundance proteins seems to have clear niche in the analytical practice. Here we investigated this opportunity through the electrochemical determination of elevated human serum albumin (HSA) in urine by HSA-imprinted MIP sensor. As a reference for a low abundance protein we used ferritin (normal levels are 12 to 300 ng/mL in the blood). In comparison up to 25 mg/L HSA in urine is considered normal and this value may increase orders of magnitude in case of kidney damage, e.g. elevated urinary excretion of albumin as in microalbuminuria[24] is an early indicator of kidney damage. Studies suggest that microalbuminuria defines a group at high risk of increased cardiovascular morbidity and mortality among patients with diabetes[25-27] or essential hypertension.[28] Moreover, microalbuminuria is associated with increased cardiovascular morbidity even in the non-diabetic, non-hypertensive population,[29] pointing out the necessity for routine screening of urinary albumin to enable prediction and prevention of future renal and cardiovascular diseases. There are many dye-binding procedures for rapid screening of elevated HSA[30] that are based on the interaction of the albumin and an anionic

dye such as bromocresol purple.[31] Since the albumin bound dye has a different absorption maximum than the free dye the HSA can be detected by simple means. However, for very specific HSA determinations clinical laboratories generally use immunoassays, e.g. immunoturbidimetric assays, or separation based methods.[32] While most separation-based methods do not cope with the requirements for high-throughput routine HSA measurements, conventional immunoassays may underestimate the urinary albumin concentration as intact albumin in urine may exist in both immunoreactive and unreactive forms.[33] Therefore, we were interested to explore the use of MIPs, that are expected to give a broader specificity than antibodies, for the quantitation of HSA in urine samples of patients showing microalbuminuria. While several electropolymerizable monomers emerged for protein imprinting applications [12] for preparing the HSA-imprinted MIP we used scopoletin as monomer, which has been introduced by Gajovich-Eichelmann[34] for the electrosynthesis of protein-MIPs and proved to enable the recognition of several protein targets.[34-38] By electropolymerization scopoletin forms an insulating polymer film, the thickness of which can be tuned to match the characteristic dimensions of the protein. The protein binding to the MIP was detected by measuring the oxidative current of a redox probe on the underlying electrode, i.e., the protein binding hinders the permeability of the redox probe through the MIP nanofilm.

2. EXPERIMENTAL

2.1. Chemicals and reagents

Scopoletin, human serum albumin (HSA) (isoelectric point (pI) 4.7), ferritin (pI 4,5), avidin (pI 10), lysozyme (pI 11.35) and sodium dodecyl sulphate (SDS) were obtained from Sigma (Steinheim, Germany). Potassium hexacyanoferrate(II) trihydrate ($K_4Fe(CN)_6 \cdot 3H_2O$), sodium

hydroxide and Tween 20 were purchased from Fluka (Buchs, Switzerland). All other chemicals used were analytical reagent grade and were used without further purification. Deionized water (DI) of 18.2 MΩ×cm resistivity prepared by a Millipore Milli-Q system was used in all experiments. Phosphate buffered saline (10 mM, pH 7.4 at 25°C, 137 mM NaCl, 2.7 mM KCl) was prepared according to the manufacturer's instructions by dissolution of one phosphate buffered saline tablet (Sigma, Steinheim, Germany) in 200 ml DI water.

2.2. Instrumentation

Electrochemical measurements were carried out with an Autolab potentiostat/galvanostat (model PGSTAT 12, Metrohm Autolab B.V, Utrecht, The Netherlands) controlled by a GPES 4.9 software package (Metrohm Autolab B.V, Utrecht, The Netherlands). A standard three electrode system was used to conduct all electrochemical experiments: a gold disk electrode (2 mm diameter) as working electrode, a Ag/AgCl/KCl (3.5 mol/dm^3) reference electrode, and a platinum wire as counter electrode. Non-specific adsorption and rebinding capacity of MIPs and NIPs were evaluated by quartz crystal microbalance (eQCM 10M™ with Reference 600 potentiostat, Gamry Instruments Inc., Warminster, USA). 10 MHz Au-coated quartz crystals (Gamry Instruments Inc., Warminster, USA) were used to prepare MIPs and NIPs for AFM and QCM measurements.

2.3. Electrosynthesis of polymer films

Molecularly imprinted polymers (MIPs) and non-imprinted polymers (NIPs) were prepared by electropolymerization of scopoletin monomer on 2 mm diameter gold disk electrodes or on 10 MHz gold-coated quartz crystals. The crystals were used as received, while the disk electrodes were cleaned before modification by polishing successively with 1.0 and 0.05 micrometer particle size alumina slurry (Buehler, Lake Bluff, USA) followed by thoroughly washing in an ultrasonic bath with DI water for 1 min. The electrode was electrochemically

cleaned afterwards by cycling the potential between -0.2 and 1.5 V in 0.1 M H_2SO_4 at 50 mV/s, until a steady cyclic voltammogram (CV) was obtained (generally 10 cycles). The electrosynthesis of imprinted polyscopoletin film was performed after optimization by CV (3 cycles) in the potential range of 0.0 to 1.0 V at a scan rate of 150 mV/s. The polymerization mixture contained 1 mM scopoletin and 7.5 μM HSA or 1 μM ferritin in PBS at pH 7.4. To remove the template from the freshly prepared MIP films, the electrode was consecutively immersed in 5 mL of gently agitated solutions of 5 mM NaOH (10 min), 5% SDS (5 min), 5 mM NaOH (10 min) for HSA, and additionally in 0.05% Tween20 (5 min), 5 mM NaOH (10 min) for ferritin, and finally in DI water for 5 minutes in both cases. The non-imprinted polymer (NIP) electrodes were prepared with the same procedure but without protein template during the electropolymerization of scopoletin.

2.4. Electrochemical detection of the MIP-target binding

The protein binding and removal process at MIP and NIP electrodes were characterized by cyclic voltammetry in 10 mM $K_4Fe(CN)_6$ in PBS at pH 7.4 in the range of -0.2 to 0.6 V at a scan rate of 50 mV/s. For protein binding the MIPs and NIPs were equilibrated in the ferrocyanide solution where a reference CV was recorded, followed by addition of HSA or ferritin. After 10 min equilibration the CV was remeasured. The response for a certain target protein concentration was determined as the difference of the oxidation current ($\Delta I = I_0 - I_t$) of the ferrocyanide before (I_0) and after the protein addition (I_t). For measuring in real samples the sensor was immersed in the urine or plasma for 10 min, followed by 10 min in PBS and rinsing. Finally, the electrode was transferred into the ferrocyanide solution to measure the CV. All experiments were performed at room temperature.

2.5. Analysis of urine and plasma samples

The practical applicability of the electrodes was tested for the quantification of HSA and ferritin in human urine and plasma samples, respectively. Spot urine samples were obtained from healthy volunteers and from diabetic patients. Depending on the content of HSA, the samples were used either undiluted or diluted 2 or 10 times with PBS pH 7.4 for analysis. Plasma from healthy donors was obtained from the Hungarian National Blood Transfusion Service. The quantitative determination of microalbumin in human urine was made by standard immunoturbidimetric method on a Beckman Coulter AU analyser.

The total protein content of urine samples was determined after desalting the urine samples (Zeba Microspin desalting columns, 7K MWCO, Thermo Fisher) following the standard or enhanced protocol (incubation at 37 or 60°C) of the Pierce BCA Protein Assay kit (Thermo Fisher). To correct for contingent losses during sample clean-up HSA standards were subjected to the same desalting protocol and the resulting HSA was measured..

2.6. Determination of the MIP and NIP thickness

The thickness of polymer films deposited on quartz crystals was measured using an atomic force microscope (AFM, FlexAFM, Nanosurf, Liestal, Switzerland). The polymer was mechanically removed over a 1x1 μm area by scanning it in contact mode using a TAP190GD-G tip (Budget Sensors, force constant: 48 N/m, length: 225 μm) with 500 nN force in five consecutive cycles. A 3×3 μm area, including the scratched area was then scanned in tapping mode and depth profiles were taken across the image.

3. RESULTS AND DISCUSSION

3.1. Electrosynthesis of the molecularly imprinted film

The first cycle during the electropolymerization of scopoletin by CV revealed a current peak at 0.5 V corresponding to the oxidation of the monomer: The oxidative current decreased with each additional cycle due to the gradual enclosing of the insulating polyscopoletin film

that hinders the access of monomers to the electrode (Figure 1 f). The complete suppression of the oxidation current at the end of the CV program suggests that the film is non-porous given that not even the small molecular weight monomer can permeate through, which is beneficial in terms of providing a highly conformal and dense polymeric matrix for protein imprinting. During electropolymerization of the MIPs, the protein molecules in the electropolymerization mixture are entrapped in the polymer matrix due to the molecular imprinting effect, i.e., given the high ionic strength of the polymerization solution most likely through formation of hydrogen bonds and hydrophobic interactions with scopoletin. After washing the MIPs to remove the template the current of the redox probe increases (Figure 1c,e) but the obtained peak currents were smaller than that on the bare gold electrode. This suggested that the polymer film remains on the electrode and only some pores were liberated by template extraction. This was confirmed by the lack of change in the current response of the NIP film subjected to the same washing procedure. Similarity between CVs for the MIPs and NIP electropolymerization indicated no electrochemical activity of HSA or ferritin within -0.2 to 0.4 V.

3.2. Optimization of the surface protein imprinting of polyscopoletin

The analytical MIP performance is expected to be influenced by the conditions of the electrodeposition and the measurement procedure. Therefore, the electrosynthesis of the MIPs in terms of thickness and physical stability of the polymer film was investigated as a function of the number of polymerization cycles and scan rate, template concentration and extraction method as well as rebinding time. The performance of the prepared polymer films was evaluated through their template rebinding properties using the template concentration dependent changes of the oxidation peak current of ferrocyanide (ΔI).

3.2.1. Effect of the electropolymerization conditions

Since polyscopoletin forms an insulating film, the polymer growth stops after a compact film is obtained, but these films can reach a few tens of nanometers in thickness.[39] Such thicknesses may already irreversibly entrap the template proteins, therefore the film thickness needs to be controlled. The main parameters of the electropolymerization affecting the thickness and the compactness of the deposited polymer films are the number of polymerization cycles and the scan rate, respectively,[12] while the concentration of the template in the polymerization cocktail is expected to influence the binding site density. In our experiments, five or more cycles led to the formation of thicker polymer films from which the template could not be extracted quantitatively (data not shown). On the other hand, films formed with only one or two cycles were too thin and were not stable during subsequent washing steps. Thus, the optimal film thickness was obtained with three polymerization cycles. The effect of scan rate on template recognition was examined in the range of 50 mV/s to 200 mV/s in the case of ferritin imprinting (Figure 2a). The lowest scan rate resulted in the formation of compact polyscopoletin film from which the template could not be removed efficiently as suggested by the low rebinding ability of this film (data not shown). The film prepared with 100 mV/s scan rate had more than twice as high sensitivity which further improved slightly with the increase of scan rate. Ultimately, 150 mV/s scan rate was chosen for further experiments.

The effect of the template concentration in the polymerization mixture was investigated by preparing MIPs with 1 to 15 μM HSA as template and measuring the response to 100 mg/dm^3 HSA. The results indicated that the response of the MIP films to HSA increased with template concentration up to 7.5 μM suggesting that an increasing number of imprints were formed in the polymer (Figure 2b). This value was chosen for subsequent experiments. Higher template concentrations led to a slight decrease in the analytical signal, which is most

likely due to surface aggregation of HSA at high concentrations, which may in fact reduce the binding site density. [40]

3.2.2. Template removal

Extraction of the template molecules liberates the binding sites formed during the MIP synthesis and is therefore a prerequisite for all subsequent binding experiments and sensing applications. For optimal template removal, several procedures were examined with regard to their ability to remove the ferritin molecules from the imprinted polymer matrix. Electrochemical template removal[41] was performed by immersing the polymer-modified electrode in 0.1 M H_2SO_4 and cycling the potential between -0.2 and 1.5 V at 200 mV/s and the CV of 10 mM $K_4Fe(CN)_6$ was obtained intermittently to monitor the progression of the template removal. A sudden increase in the peak current was observed between 30 and 40 removal cycles indicating the necessity to perform at least 40 cycles to quantitatively remove the template (Figure 3a). On the other hand, the NIP film remained impermeable to the redox probe even after 70 cycles confirming that the polymer itself is intact. Unfortunately, the procedure was not reproducible for all conditions and gradual degradations of the polymer film turned us to seek milder conditions for template removal.

Therefore, template removal was attempted by enzymatic digestion of the template using 500 mg/dm^3 proteinase K (in 10 mM NH_4OAc pH 8 + 5 mM $CaCl_2$) during gently shaking. Proteinase K has a broad cleavage specificity that results in very small peptide fragments or even single amino acids[42] which are then expected to be easily removed from the polymer. However, we found that this mild treatment, i.e., 1h incubation with the enzyme, is insufficient for the complete template removal while longer times were impractical. Nevertheless, the enzyme digestion may still be considered when the template removal is

performed simultaneously as the last step of MIP fabrication on a large batch of sensors (e.g. mass produced microfabricated electrodes).

The enzyme digestion was complemented with further intensive washing sequence with 5 mM NaOH, 5% SDS and 5 mM NaOH (Figure 3b), which was found to be efficient. However, since this post-treatment setbacks the benefits of the mild enzymatic digestion we explored the possibility to remove the template solely by washing the electrodes in the mentioned solutions. We found that 10 min washing in 5 mM NaOH followed by 5 min in 5% SDS and 10 min in 5 mM NaOH was equally or even more effective (Figure 3b, red curve) as the same sequence applied after digestion. Further testing of various washing solutions including 5 mM H_2SO_4, 0.05% Tween20, ethanol and PBS confirmed that for HSA-MIPs, the above mentioned sequence was the most effective, while ferritin was best removed by this sequence followed by an additional 5 min in 0.05% Tween 20 and 5 min in 5 mM NaOH. In both cases, the washing procedure was completed by rinsing the electrodes in water.

3.2.3. Template rebinding

The time required to reach a steady sensor response in a given analyte solution was determined by equilibrating the electrodes in 10 mM $K_4Fe(CN)_6$ solution in PBS (pH 7.4) followed by addition of 1 g/dm^3 ferritin or 150 mg/dm^3 HSA. The sensor response (CV curve) was then periodically recorded over a time range of at least 35 minutes. The peak current of ferrocyanide oxidation decreased rapidly with the increase of incubation time (ΔI increased, Figure 4.) as the template molecules rebound to the MIP blocked the electron transfer between the electrode and the redox probe. A steady cyclic voltammogram indicating that the rebinding equilibrium is reached was obtained after 35 min for the ferritin-imprinted polymer. However, the signal did not change significantly after 20 min which therefore was

chosen for further experiments to minimize the analysis time. In the case of HSA an incubation time of 10 minutes was sufficient. Furthermore, we found that adding the analyte directly to the ferrocyanide solution or incubating the electrode in a separate solution with the analyte for the same duration and then transferring it into ferrocyanide solution did not affect the response (data not shown). Therefore, the simpler, additive method was applied to construct calibration curves, while the selectivity and biological sample measurements were performed in separate solutions to remove by rinsing unbound interferents.

3.3. Surface characterization

The thickness of the polymer films was determined by mechanically removing them from the gold over a rectangular area by using AFM in contact mode then remapping the surface in tapping mode[19]. Representative depth profiles taken across the indented area reveal a polymer film thickness close to 3 nm for the non-imprinted and 12-14 nm for the ferritin-imprinted film (Figure 5). Protein sensing with the surface imprinted polymer-modified electrodes

3.3.1. Concentration dependence and limit of detection

To investigate the concentration dependence of the response of HSA and ferritin-imprinted polymers, the background solution containing 10 mM $K_4Fe(CN)_6$ in PBS was spiked with various amounts of the target proteins and the CV of the redox probe was recorded after each protein addition. The analytical response of the sensors, i.e. the change in oxidation current of ferrocyanide (ΔI) in relation with the concentration of the target proteins is shown in Figure 6. A close to linear range was observed between 20 and 100 mg/dm^3 for HSA while the dynamic range of the ferritin sensor was between 40 and 360 mg/dm^3. The HSA and ferritin imprinted MIPs showed saturation around 400 (ca. 6 μM) and 600 mg/dm^3 (ca. 1.3 μM)

respectively. The limit of detection, calculated as $3 \cdot \sigma_{intercept}$/slope from the parameters of a linear fitting to the lowest concentration ranges, was found to be 3.7 mg/dm^3 (56 nM) for HSA and 10.7 mg/dm^3 (10 nM) for ferritin. Interestingly the 5-6 times lower saturation concentration and LOD in case of ferritin seems to match roughly the ratio in the footprints of the two molecules, i.e., the spherical shape ferritin has a radius of 9.1 nm[43] while HSA 3.51 nm[44] which means that the ratio of their footprints is 3.9. The HSA response could be well fitted (adjusted R-square of 0.986) with the Hill equation having the Hill coefficient (n) indicative of binding cooperativity set to 1, which resulted in a K_d of 2.8 (± 0.4) μM.

The NIP electrodes were practically impenetrable for the redox probe and consequently showed only a very low response even to high concentrations of HSA or ferritin (data not shown). However, QCM measurements confirmed that increasing concentrations of HSA did not provoke any frequency changes suggesting that non-specific adsorption was negligible (data not shown).

3.3.2. Repeatability and stability

The repeatability of the HSA-MIP and ferritin-MIP modified electrodes was determined at 150 mg/dm^3 HSA and 100 mg/dm^3 ferritin concentration levels in five subsequent template binding-removal cycles, respectively. The relative standard deviation of the HSA and ferritin sensors was 6.8% and 6.3%, respectively, demonstrating the possibility to regenerate and repeatedly use the MIP-based sensors. The reproducibility of the sensor fabrication was tested by preparing four MIP-coated electrodes under the same conditions and measuring their additive response to 50-250 mg/dm^3 HSA. The relative standard deviation of the sensitivities was 5.8%, which matched within the experimental error the repeatability of the MIP-based sensors. The short term stability was evaluated by keeping the MIP-based electrode in DI water for seven days and measuring intermittently its response to 100 mg/dm^3

HSA or 200 mg/dm^3 ferritin. The largest deviation from the original response was 5.7% and 8%, respectively, over the studied time range.

3.3.3. Selectivity

A quick assessment of the selectivity of the HSA-sensor towards proteins was made beside ferritin (much larger than HSA, MW 450 kDa) with avidin (similar size as HSA) and lysozyme (considerably smaller size than HSA) at 100 mg/dm^3 level. Since the polyscopoletin film is negatively charged and the latter two proteins with high pIs are notorious for their nonspecific adsorption they were expected to be indicative of the worst scenario, i.e., highest nonspecific adsorption.[35] After immersed in the examined protein solutions for 5 min, the sensor was washed with deionised water and then CV experiments were performed in 10 mM $K_4Fe(CN)_6$ in PBS. As shown in Figure 7a the sensor response to avidin and lysozyme was less than 30% of the response given to the same concentration of HSA. As expected the much larger ferritin (450 kDa) with a pI of 5.5 produced the smallest interference.

To eliminate the eventuality that electroactive molecules such as ascorbic acid and uric acid are interfering with the current signal, i.e., adsorbed during incubation in the sample on the MIP which may interfere with the ferrocyanide signal, the MIP modified electrodes were incubated in 5.7 mM ascorbic acid and 4.5 mM uric acid and then subjected to the same short washing procedure as in case of protein detection. Cycling the potential of the electrodes in ferrocyanide solution the observed change in the current observed was less than 6% indicating that they were easily removed from the cavities of the MIP during the rinsing step (Figure 7b).

3.4. Urine albumin and plasma ferritin measurements

The ferritin levels in the plasma of healthy patients range from 12 to 300 μg/dm^3 while the LOD of MIP based ferritin sensor is 40 mg/dm^3. Thus this MIP sensor is clearly not suitable for clinical application. However, to check the assumption that high abundance proteins may be determined even in complex samples we spiked the plasma with ferritin concentrations (40-150 mg/dm^3) assessable with the ferritin-MIP-based electrode. The recoveries were surprisingly good given the complexity of the matrix, i.e. within 5% except for the smallest tested concentration where ca. 20 % error was observed, most likely due to uncertainty of the measurements close to the LOD (Table 1).

On the other hand, albumin is the most abundant protein in blood being present in 35-50 g/dm^3 concentration and it can also appear in the urine in up to 25 mg/dm^3 concentration for healthy individuals. In case of microalbuminuria the urinary albumin excretion elevates further to ca. 200 mg/dm^3, which can be an early indicator of kidney damage. Given its operating range of 20 to 300 mg/dm^3 these level should be readily accessible with HSA-MIP based sensor. First a spot urine sample from a healthy volunteer was measured where the albumin concentration was found to be below the limit of detection. The sample was then spiked with 20-120 mg/dm^3 albumin and the added concentrations could be determined with less than 5% relative error (Table 2) indicating that the sensor is suitable for rapid testing of albumin in urine.

In order to further evaluate the applicability and reliability of the developed MIP sensor device in clinical analysis, three urine samples from diabetic patients were analysed directly or after dilution with PBS pH 7.4. The electrodes were incubated for 5 min in the urine samples and after washing CV experiments were performed in 10 mM $K_4Fe(CN)_6$ dissolved in PBS to determine the oxidation current. Quantification of HSA was performed using the multiple standard addition method and the results were compared with albumin levels determined with a standard immunoturbidimetric method. The results show less than 10 %

deviation between the HSA contents determined by the two methods (Table 3), which given the general uncertainties of HSA measurements, i.e., HSA present in various forms and molecular associates seems satisfactory. To further show that the MIPs are selectively determining the HSA content of the samples the total protein content of the urine samples were estimated by the BCA assay. The total protein content was found to be significantly higher than the HSA content for each sample, suggesting that the HSA-MIP can be used to determine the HSA in urine in the presence of other proteins as well.

4. CONCLUSIONS

In this study we have shown that polyscopoletin nanofilms can be made sensitive to two different proteins, HSA and ferritin, by surface imprinting. These MIPs were rendered selective only by the imprinting process as the employed monomers and proteins had no distinct features to predestine the formation of binding sites with strong interaction with the template. Indeed, the K_d of the HSA-imprinted film was in the lower micromolar range, while the saturation concentration and LODs of the two MIPs indicates fairly similar responses scaling mainly with the size of the template proteins. As expected the relatively high LODs obtained (10.7 mg/dm^3 for ferritin) did not allow the assessment of endogenous ferritin in blood. However, ferritin spiked plasma samples falling in the dynamic range of the ferritin-MIP have shown excellent recoveries, despite the complexity of the matrix. On the other hand, the more prevalent albumin was successfully quantified with the HSA-MIP-based sensor in urine samples from diabetic patients. The results were in satisfactory agreement with immunoturbidimetric determination, suggesting that this approach can be used for detection of HSA in urine sample for diagnostic purposes as alternative to more expensive antibody based assays. This application seems to not require extremely high affinity MIPs[22] as reported earlier and overall suggests as a perspective application for genuine

"randomly" imprinted protein MIPs the quantification of high abundance proteins of clinical relevance that, however, still require a selective recognition process.

Acknowledgement

This work was supported by the Lendület program of the Hungarian Academy of Sciences (LP2013-63) and ERA-Chemistry (2014, 61133; OTKA NN117637). Z.S. acknowledges scholarship from the Ministry of Education, Science and Technological Development of the Republic of Serbia for post-doc research stay at the Budapest University of Technology and Economics (in the frame of Project TR 31014).

References

[1] M. Menger, A. Yarman, J. Erdőssy, H.B. Yildiz, R.E. Gyurcsányi, F.W. Scheller, MIPs and Aptamers for Recognition of Proteins in Biomimetic Sensing, Biosensors-Basel, 6 (2016).
[2] G. Wulff, A. Sarhan, Über die Anwendung von enzymanalog gebauten Polymeren zur Racemattrennung, Amgew. Chem. In. Ed., 84 (1972) 364-364.
[3] R. Arshady, K. Mosbach, Synthesis of substrate-selective polymers by host-guest polymerization, Die Makromolekulare Chemie, 182 (1981) 687-692.
[4] H. Nishino, C.-S. Huang, K.J. Shea, Selective Protein Capture by Epitope Imprinting, Amgew. Chem. In. Ed., 45 (2006) 2392-2396.
[5] A. Rachkov, N. Minoura, Recognition of oxytocin and oxytocin-related peptides in aqueous media using a molecularly imprinted polymer synthesized by the epitope approach, J. Chromat. A, 889 (2000) 111-118.
[6] Y. Li, H.-H. Yang, Q.-H. You, Z.-X. Zhuang, X.-R. Wang, Protein Recognition via Surface Molecularly Imprinted Polymer Nanowires, Anal. Chem., 78 (2006) 317-320.
[7] A. Menaker, V. Syritski, J. Reut, A. Öpik, V. Horváth, R.E. Gyurcsányi, Electrosynthesized Surface-Imprinted Conducting Polymer Microrods for Selective Protein Recognition, Adv. Mater., 21 (2009) 2271-2275.
[8] G. Lautner, J. Kaev, J. Reut, A. Opik, J. Rappich, V. Syritski, R.E. Gyurcsanyi, Selective Artificial Receptors Based on Micropatterned Surface-Imprinted Polymers for Label-Free Detection of Proteins by SPR Imaging, Adv. Funct. Mater., 21 (2011) 591-597.
[9] O. Hayden, P.A. Lieberzeit, D. Blaas, F.L. Dickert, Artificial Antibodies for Bioanalyte Detection—Sensing Viruses and Proteins, Adv. Funct. Mater., 16 (2006) 1269-1278.
[10] H. Shi, W.B. Tsal, M.D. Garrison, S. Ferrari, B.D. Ratner, Template-imprinted nanostructured surfaces for protein recognition, Nature, 398 (1999) 593-597.
[11] D.R. Kryscio, M.Q. Fleming, N.A. Peppas, Conformational studies of common protein templates in macromolecularly imprinted polymers, Biomed. Microdevices, 14 (2012) 679-687.

[12] J. Erdőssy, V. Horváth, A. Yarman, F.W. Scheller, R.E. Gyurcsányi, Electrosynthesized molecularly imprinted polymers for protein recognition, Trac-Trend Anal Chem, 79 (2016) 179-190.
[13] A. Tretjakov, V. Syritski, J. Reut, R. Boroznjak, A. Opik, Molecularly imprinted polymer film interfaced with Surface Acoustic Wave technology as a sensing platform for label-free protein detection, Anal. Chim. Acta, 902 (2016) 182-188.
[14] A. Tretjakov, V. Syritski, J. Reut, R. Boroznjak, O. Volobujeva, A. Opik, Surface molecularly imprinted polydopamine films for recognition of immunoglobulin G, Microchim Acta, 180 (2013) 1433-1442.
[15] M. Menger, A. Yarman, J. Erdőssy, H.B. Yildiz, R.E. Gyurcsányi, F.W. Scheller, MIPs and aptamers for recognition of proteins in biomimetic sensing, Biosensors, 6 (2016).
[16] D. Cai, L. Ren, H.Z. Zhao, C.J. Xu, L. Zhang, Y. Yu, H.Z. Wang, Y.C. Lan, M.F. Roberts, J.H. Chuang, M.J. Naughton, Z.F. Ren, T.C. Chiles, A molecular-imprint nanosensor for ultrasensitive detection of proteins, Nat Nanotechnol, 5 (2010) 597-601.
[17] B.V.M. Silva, B.A.G. Rodriguez, G.F. Sales, M.D.T. Sotomayor, R.F. Dutra, An ultrasensitive human cardiac troponin T graphene screen-printed electrode based on electropolymerized-molecularly imprinted conducting polymer, Biosens. Bioelectron., 77 (2016) 978-985.
[18] D. Dechtrirat, N. Gajovic-Eichelmann, F.F. Bier, F.W. Scheller, Hybrid Material for Protein Sensing Based on Electrosynthesized MIP on a Mannose Terminated Self-Assembled Monolayer, Adv. Funct. Mater., 24 (2014) 2233-2239.
[19] K.J. Jetzschmann, G. Jagerszki, D. Dechtrirat, A. Yarman, N. Gajovic-Eichelmann, H.D. Gilsing, B. Schulz, R.E. Gyurcsanyi, F.W. Scheller, Vectorially Imprinted Hybrid Nanofilm for Acetylcholinesterase Recognition, Adv. Funct. Mater., 25 (2015) 5178-5183.
[20] P. Jolly, V. Tamboli, R.L. Harniman, P. Estrela, C.J. Allender, J.L. Bowen, Aptamer-MIP hybrid receptor for highly sensitive electrochemical detection of prostate specific antigen, Biosensors & Bioelectronics, 75 (2016) 188-195.
[21] H.J. Chen, Z.H. Zhang, L.J. Luo, S.Z. Yao, Surface-imprinted chitosan-coated magnetic nanoparticles modified multi-walled carbon nanotubes biosensor for detection of bovine serum albumin, Sensor Actuat B-Chem, 163 (2012) 76-83.
[22] M. Cieplak, K. Szwabinska, M. Sosnowska, B.K.C. Chandra, P. Borowicz, K. Noworyta, F. D'Souza, W. Kutner, Selective electrochemical sensing of human serum albumin by semi-covalent molecular imprinting, Biosens. Bioelectron., 74 (2015) 960-966.
[23] T. Matsunaga, T. Hishiya, T. Takeuchi, Surface plasmon resonance sensor for lysozyme based on molecularly imprinted thin films, Anal. Chim. Acta, 591 (2007) 63-67.
[24] T.J. Peters, 6 – Clinical Aspects: Albumin in Medicine, in: T.J. Peters (Ed.) All About Albumin. Biochemistry, Genetics and Medical Applications, Academic Press, San Diego, CA, USA, 1995, pp. 251-284.
[25] U. Weis, B. Turner, J. Gibney, G.F. Watts, V. Burke, K.M. Shaw, M.H. Cummings, Long-term predictors of coronary artery disease and mortality in type 1 diabetes, Qjm-Mon J Assoc Phys, 94 (2001) 623-630.
[26] M.B. Mattock, D.J. Barnes, G. Viberti, H. Keen, D. Burt, J.M. Hughes, A.P. Fitzgerald, B. Sandhu, P.G. Jackson, Microalbuminuria and coronary heart disease in NIDDM - An incidence study, Diabetes, 47 (1998) 1786-1792.
[27] D.K. McGuire, Influence of proteinuria on long-term outcome among patients with diabetes: The evidence continues to accumulate, Am Heart J, 139 (2000) 934-935.
[28] A. Jager, P.J. Kostense, H.G. Ruhe, R.J. Heine, G. Nijpels, J.M. Dekker, L.M. Bouter, C.D.A. Stehouwer, Microalbuminuria and peripheral arterial disease are independent

predictors of cardiovascular and all-cause mortality, especially among hypertensive subjects - Five-year follow-up of the Hoorn study, Arterioscl Throm Vas, 19 (1999) 617-624.
[29] H.L. Hillege, W.M.T. Janssen, A.A.A. Bak, G.F.H. Diercks, D.E. Grobbee, H.J.G.M. Crijns, W.H. van Gilst, D. de Zeeuw, P.E. de Jong, P.S. Grp, Microalbuminuria is common, also in a nondiabetic, nonhypertensive population, and an independent indicator of cardiovascular risk factors and cardiovascular morbidity, J Intern Med, 249 (2001) 519-526.
[30] M.L. Bishop, E.P. Fody, L.E. Schoeff, Clinical chemistry : techniques, principles, correlations, 6th ed., Wolters Kluwer Health/Lippincott Williams & Wilkins, Philadelphia, 2010.
[31] A.E. Pinnell, B.E. Northam, New automated dye-binding method for serum albumin determination with bromcresol purple, Clin. Chem, 24 (1978) 80.
[32] W.D. Comper, T.M. Osicka, Detection of urinary albumin, Advances in Chronic Kidney Disease, 12 (2005) 170-176.
[33] W.D. Comper, T.M. Osicka, G. Jerums, High prevalence of immuno-unreactive intact albumin in urine of diabetic patients, American Journal of Kidney Diseases, 41 (2003) 336-342.
[34] D. Dechtrirat, K.J. Jetzschmann, W.F.M. Stocklein, F.W. Scheller, N. Gajovic-Eichelmann, Protein Rebinding to a Surface-Confined Imprint, Adv. Funct. Mater., 22 (2012) 5231-5237.
[35] M. Bosserdt, J. Erdőssy, G. Lautner, J. Witt, K. Kohler, N. Gajovic-Eichelmann, A. Yarman, G. Wittstock, F.W. Scheller, R.E. Gyurcsányi, Microelectrospotting as a new method for electrosynthesis of surface-imprinted polymer microarrays for protein recognition, Biosensors & Bioelectronics, 73 (2015) 123-129.
[36] M. Bosserdt, N. Gajovic-Eichelman, F.W. Scheller, Modulation of direct electron transfer of cytochrome c by use of a molecularly imprinted thin film, Anal. Bioanal. Chem., 405 (2013) 6437-6444.
[37] L. Peng, A. Yarman, K.J. Jetzschmann, J.H. Jeoung, D. Schad, H. Dobbek, U. Wollenberger, F.W. Scheller, Molecularly Imprinted Electropolymer for a Hexameric Heme Protein with Direct Electron Transfer and Peroxide Electrocatalysis, Sensors-Basel, 16 (2016).
[38] A. Yarman, D. Dechtrirat, M. Bosserdt, K.J. Jetzschmann, N. Gajovic-Eichelmann, F.W. Scheller, Cytochrome c-Derived Hybrid Systems Based on Moleculary Imprinted Polymers, Electroanal, 27 (2015) 573-586.
[39] R.E. Gyurcsányi, A. Cristalli, G. Nagy, L. Nagy, C. Corder, B.D. Pendley, S. Ufer, H.T. Nagle, M.R. Neuman, E. Lindner, Analytical performance characteristics of thin and thick film amperometric microcells, Fresen. J. Anal. Chem., 369 (2001) 286-294.
[40] A. Fatoni, A. Numnuam, P. Kanatharana, W. Limbut, P. Thavarungkul, A novel molecularly imprinted chitosan-acrylamide, graphene, ferrocene composite cryogel biosensor used to detect microalbumin, Analyst, 139 (2014) 6160-6167.
[41] S.K. Mamo, J. Gonzalez-Rodriguez, Development of a Molecularly Imprinted Polymer-Based Sensor for the Electrochemical Determination of Triacetone Triperoxide (TATP), Sensors-Basel, 14 (2014) 23269-23282.
[42] W. Ebeling, N. Hennrich, M. Klockow, H. Metz, H.D. Orth, H. Lang, Proteinase K from Tritirachium album Limber, Eur. J. Biochem., 47 (1974) 91-97.
[43] T. Jøssang, J. Feder, E. Rosenqvist, Photon correlation spectroscopy of human IgG, J. Protein Chem., 7 (1988) 165-171.

[44] J.K. Armstrong, R.B. Wenby, H.J. Meiselman, T.C. Fisher, The Hydrodynamic Radii of Macromolecules and Their Effect on Red Blood Cell Aggregation, Biophys. J., 87 (2004) 4259-4270.

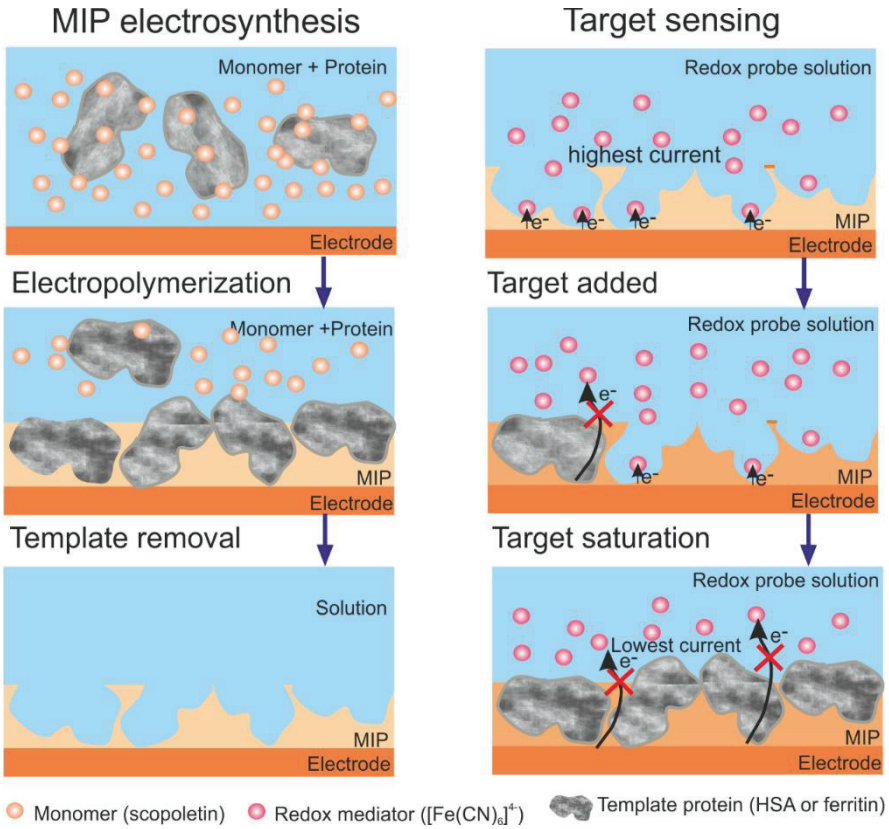

Scheme 1. Schematics of the electrosynthesis of surface imprinted polyscopoletin nanofilm on a gold electrode surface and its use for the detection of the target. Please note that while not indicated in the scheme, in case of biological samples the MIP-modified electrodes were first incubated in these samples and after washing the electrode was transferred in the redox probe solution for the measurement.

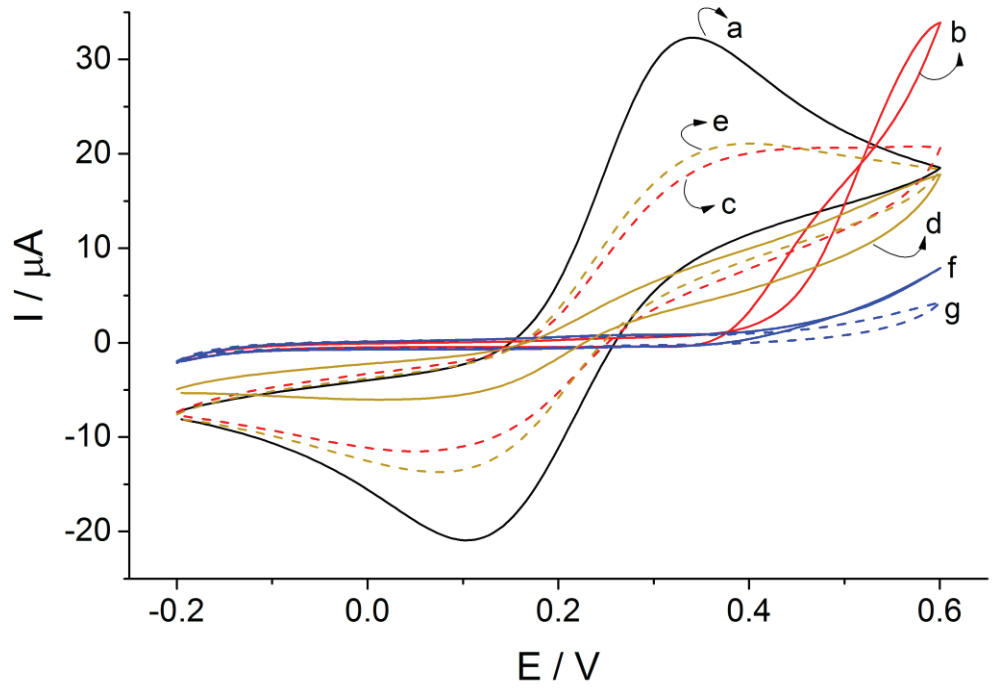

Figure 1. Cyclic voltammograms of 10 mM $K_4Fe(CN)_6$ redox probe in 10 mM PBS pH 7.4 recorded on bare Au disk electrode (a), on a MIP film coated electrode before (b,d) and after (c,e) removal of the HSA and ferritin template, respectively, and NIP film coated electrode before (f) and after washing (g).

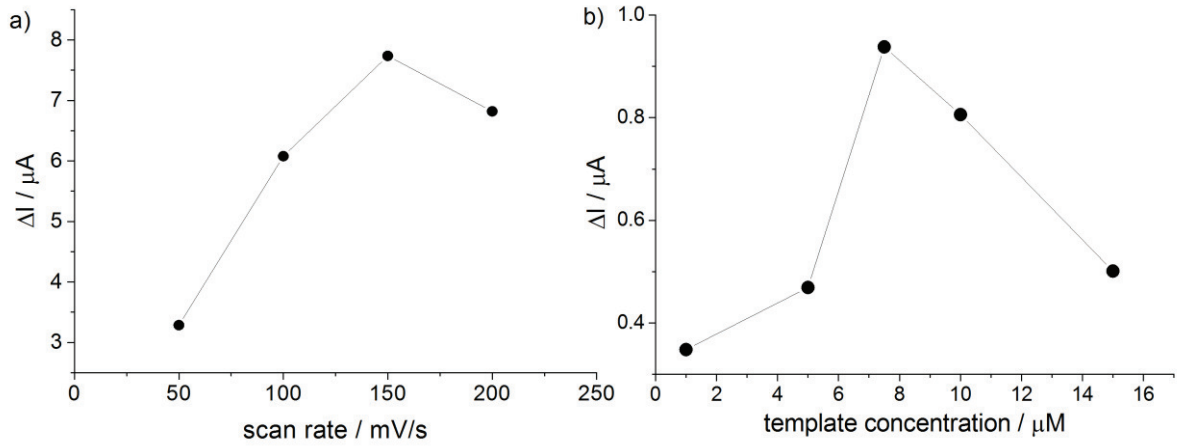

Figure 2. Effect of (a) scan rate during electropolymerization and (b) template concentration on the response of MIP-based sensors. (a) The polymers were deposited from 1 mM scopoletin in PBS pH 7.4 containing 1 μM ferritin by 3 cycles between 0 and 1 V with the specified scan rates. The sensor responses to 1 mM ferritin were measured after template removal. (b) The polymers were deposited from 1 mM scopoletin in PBS pH 7.4 containing 1-15 μM HSA by 3 cycles between 0 and 1 V at 150 mV/s. The sensor responses to 100 mg/dm^3 HSA were measured after template removal.

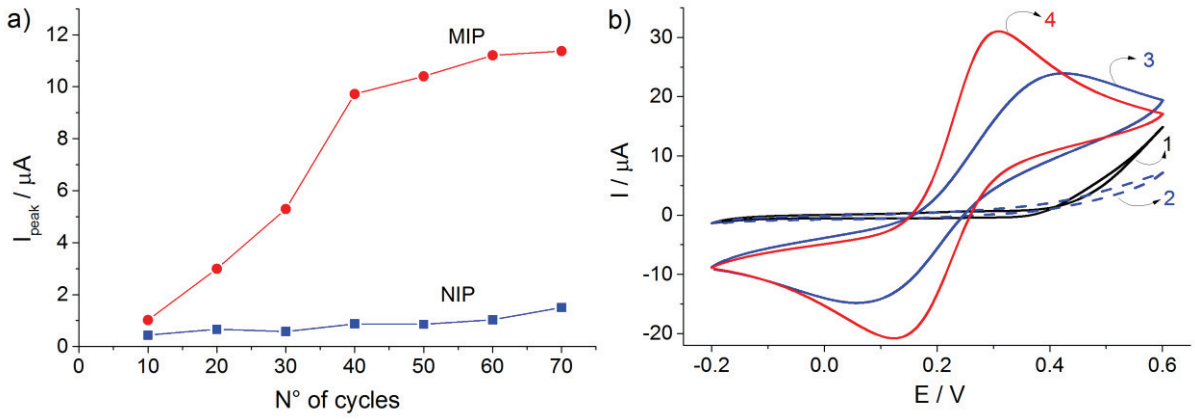

Figure 3. Removal of ferritin template by electrochemical cycling in 0.1 M H_2SO_4 (a) and by digestion with 500 mg/dm^3 proteinase K (b). (a) Oxidation peak current of 10 mM $K_4Fe(CN)_6$ with the MIP (circle) and NIP (square) covered electrodes after up to 70 cycles in H_2SO_4. (b) CVs of 10 mM $K_4Fe(CN)_6$ on MIP after polymer deposition (1-black), after 1h in proteinase K (2-dashed blue), further washed with 5 mM NaOH and 5% SDS (3- solid blue), a MIP only washed with 5 mM NaOH and 5% SDS (4- red).

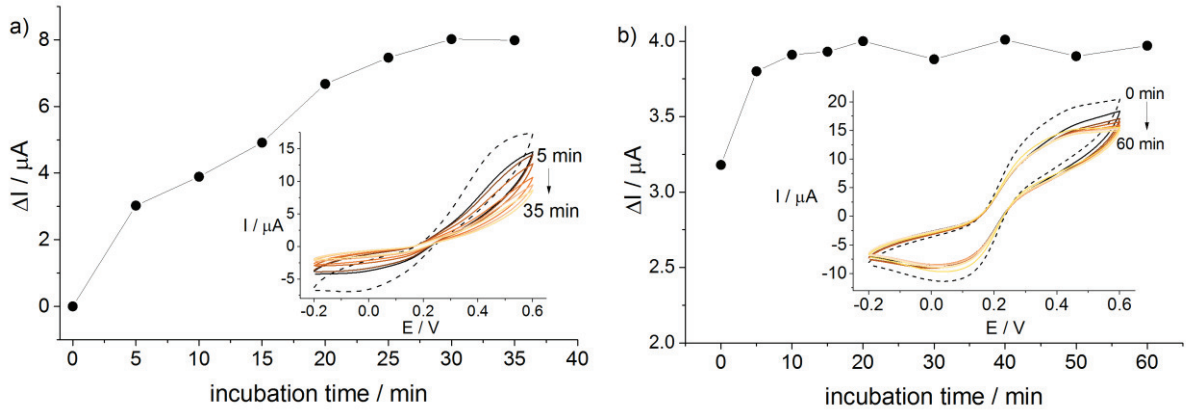

Figure 4. Effect of incubation time on the response of ferritin (a) and HSA (b) imprinted polymers to template rebinding. Insets: CVs of MIP-modified electrode before protein addition (dashed line) and after different incubation times in 1 g/dm^3 ferritin (a) or in 150 mg/dm^3 HSA (b). The CVs were recorded in 10 mM $K_4Fe(CN)_6$ (PBS pH 7.4).

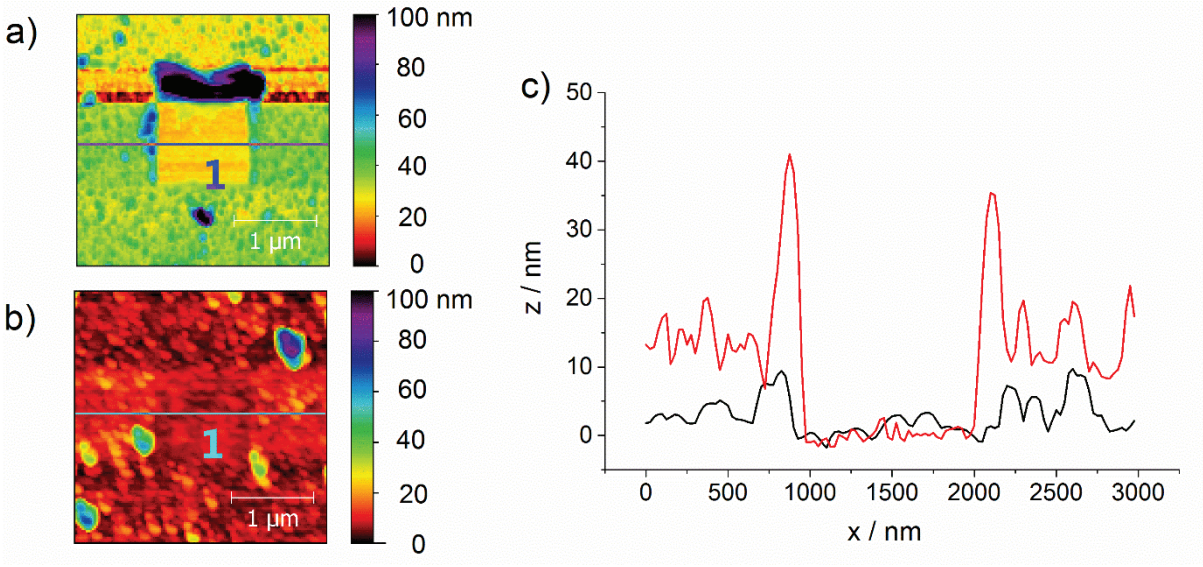

Figure 5. Representative morphology of the ferritin-imprinted (a) and non-imprinted (b) polymer layer after removing the film by contact mode AFM over a 1×1 µm area and the corresponding cross-sectional profiles (c, MIP: red, NIP: black). The polymers were deposited from 1 mM scopoletin in PBS pH 7.4, (containing additionally 1 µM ferritin in the case of MIP) by 3 potential cycles between 0 and 1 V at 150 mV/s. A TAP190GD-G tip (force constant: 48 N/m, length: 225 µm) was used for five consecutive scans in contact mode (500 nN force) to remove the polymer layers, followed by scanning a larger (3×3 µm) area in tapping mode.

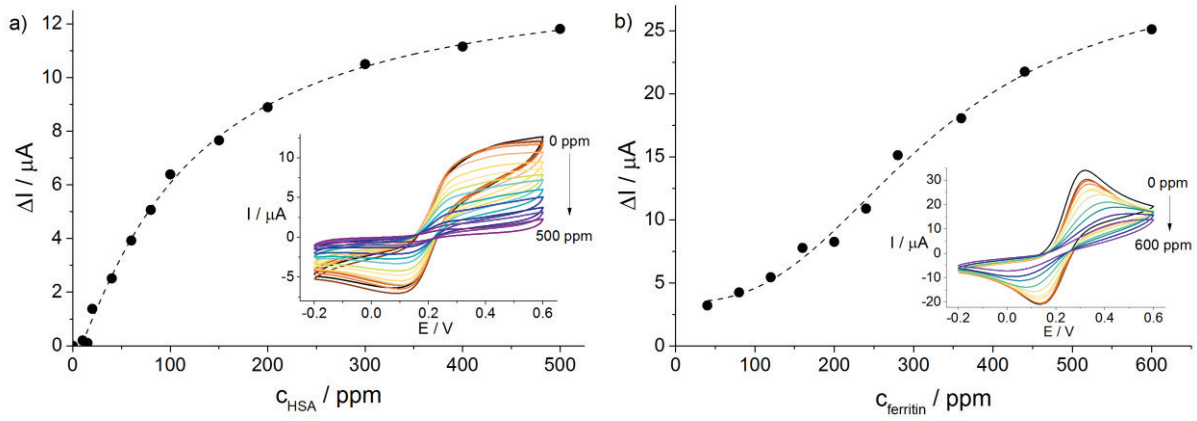

Figure 6. Concentration dependence of sensor response: 5-300 mg/dm^3 HSA rebinding to a HSA-imprinted sensor (a) and 40-600 mg/dm^3 ferritin rebinding to a ferritin-imprinted sensor (b). Insets: corresponding CV curves in 10 mM $K_4Fe(CN)_6$ in PBS.

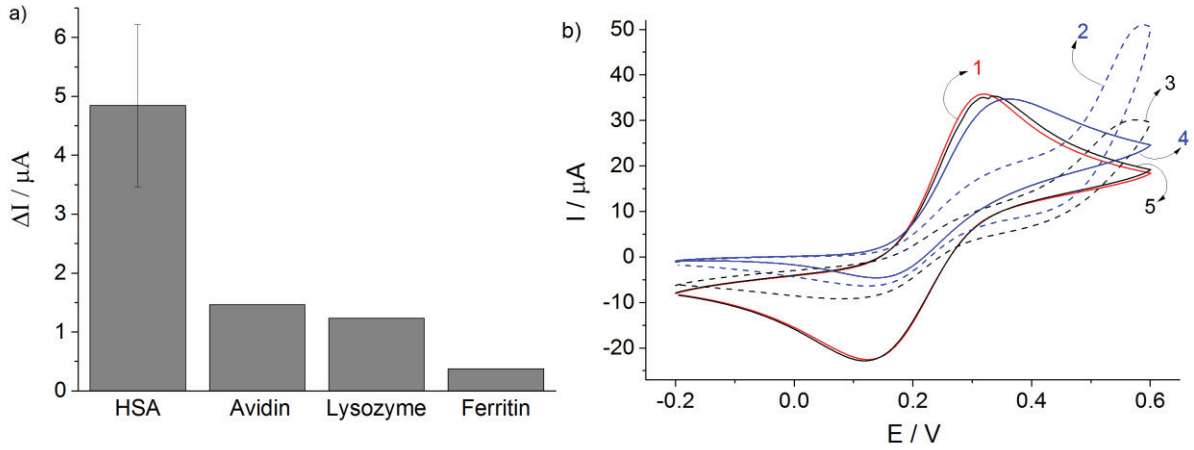

Figure 7. The HSA-MIP based sensor's response to (a) various proteins at 100 ppm concentration level and (b) small molecules: CV curve of 10 mM $K_4Fe(CN)_6$ in PBS pH 7.4 on HSA-imprinted MIP electrode before (1-red) and after incubation in 5.7 mM ascorbic acid (2-dashed blue) or 4.5 mM uric acid (3-dashed black) and after subsequent washing (after ascorbic acid: 4-solid blue, after uric acid: 5-solid black).

Table 1. Determination of ferritin in spiked plasma samples

added concentration, mg/dm^3	determined concentration, mg/dm^3	recovery, %
40	48.4	121.0
60	62.8	104.7
80	83.2	104.0
100	103.9	103.9
120	128.6	107.2
150	154.2	102.8

Table 2. Determination of albumin in spiked spot urine samples

added concentration, mg/dm^3	determined concentration[a], mg/dm^3	recovery, %
20	20.93±1.48	104.7
60	62.98±2.36	105.0
80	83.57±3.45	104.5
100	125.78±5.02	104.8

[a] mean±2SD, n=3

Table 3. Determination of HSA in urine samples obtained from diabetic patients

Sample	MIP (mg/L)	Immunoturbidimetry (mg/L)	Relative error (%)	Total protein (mg/mL)
1	86.0	89.2	3.7	165
2	7.7	8.3	8.8	107
3	546.2	506.5	7.83	728